The role of phosphorylation and dephosphorylation in the regulation of Rubisco activase

Nikita Bhatnagar[a], , 0000-0001-7832-1347
Sarah S. Chung[a,b], sohyeon2@illinois.edu, 0009-0005-6096-5343
John Hodge[a,b], jghodge@illinois.edu, 0000-0003-0793-1871
Ryan A Boyd[a,b], raboyd2@illinois.edu, 0000-0003-4009-7700
Sang Yeol Kim[b]
Mia Sands[b], xin7@illinois.edu, 0000-0002-4925-9772
Andrew D. B. Leakey[a,b,c], leakey@illinois.edu, 0000-0001-6251-024X
Donald R. Ort[a,b,c], d-ort@illinois.edu, 0000-0002-5435-4387
Steven Burgess[a,b], sjb287@illinois.edu, 0000-0003-2353-7794

Affiliations
[a]Carl R. Woese Institute for Genomic Biology, University of Illinois Urbana-Champaign
[b]Department of Plant Biology, University of Illinois Urbana-Champaign
[c]Department of Crop Sciences, University of Illinois Urbana-Champaign

Corresponding Author: Steven J. Burgess
The author responsible for distribution of materials integral to the findings presented in this article in accordance with the policy described in the Instructions for Authors (https://academic.oup.com/plphys/pages/General-Instructions) is (insert author name).

Running head:
Role of phosphorylation/dephosphorylation the regulation of of Rubisco activase

SUMMARY
Rubisco activase is an ATP-dependent chaperone that facilitates dissociation of inhibitory sugar phosphates from the catalytic sites of ribulose-1,5-bisphosphate carboxylase/oxygenase during photosynthesis. In Arabidopsis, Rubisco activase is negatively regulated by dark-dependent phosphorylation of threonine 78. Here we identify chloroplast localized *SHEWENELLA-LIKE PROTEIN PHOSPHATASE 1 (SLP1)* as the major phosphatase responsible for light-dependent dephosphorylation of Rubisco activase. The prevalence of threonine 78 in Rubisco activase was investigated across sequences from 91 plant species, finding 29 (~32%) species shared a threonine in the same position. Analysis of seven C3 species with an antibody raised against a threonine 78 phospho-peptide demonstrated that this position is phosphorylated in multiple genera. However, light-dependent dephosphorylation of threonine

78 was observed only in Arabidopsis. Further, phosphorylation of threonine 78 could not be detected in any of the four C4 grass species examined. The results suggest that despite conservation of threonine 78 in Rubisco activase from a wide range of species, a regulatory role for phosphorylation at this site is more limited. This provides a case study for how variation in post-translational regulation can amplify functional divergence across the phylogeny of plants beyond what is explained by sequence variation in a metabolically important protein.

INTRODUCTION

Rubisco catalyzes the addition of CO_2 to a molecule of ribulose-1,5-bisphosphate (RuBP) forming two molecules of 3-phosoglycerate (3-PGA) and in many circumstances is the rate limiting step of CO_2 assimilation (Stitt *et al.*, 1991; Hudson *et al.*, 1992; Stitt & Schulze, 1994; Poolman *et al.*, 2000; Zhu *et al.*, 2007). To perform this reaction the enzyme must first be activated through attachment of CO_2 to a catalytic lysine in order to bind Mg^{2+} (Lorimer and Miziorko, 1980). However, the enzyme is susceptible to inhibition by attachment of RuBP prior to activation, or binding of one of several inhibitory sugar phosphates to the active site (Orr et al., 2023). Inhibitors can be released by the action of Rubisco activase (Rca) (Somerville et al., 1982; Salvucci et al., 1986; Jiang et al., 1994), which uses energy from ATP hydrolysis to drive conformational changes in Rubisco, freeing the active site (Neuwald et al., 1999; Portis & Jr., 2003; Flecken et al., 2020). Therefore Rca is critical for regulation of Rubisco activity and carbon assimilation (Parry et al., 2013; Wijewardene et al., 2021; Qu et al., 2023; Orr et al., 2023).

Rca itself is subject to regulation, which provides a link between carbon assimilation and electron transport. Most of our understanding about this process comes from Arabidopsis, where there are two isoforms of Rca which differ in size. The longer 'α' isoform possesses a 20-30 amino acid C-terminal extension (To et al., 1999) which contains two cysteine residues (Cys-451 and Cys-470). The cysteines are regulated by thioredoxin f in response to changes in the ATP/ADP arising from variation in rates of electron transport and ATP synthesis (Zhang & Portis, 1999b; Zhang et al., 2002). In the dark, the cysteines are oxidized to form a disulfide bridge (oxidized state, E_m ~344 mV pH 7.9)(Hutchison et al., 2000), increasing the sensitivity of Rca to inhibition by ADP (Portis et al., 2007), downregulating Rca activity and CO_2 fixation. However, redox regulation of Rca does not appear to be essential. Solanaceae species, such as tobacco, are reported to only express Rca-β, which lacks the C-terminal extension, (Nagarajan & Gill, 2018), and the sensitivity of Rca-β isoforms to inhibition by ADP varies (Carmo-Silva & Salvucci, 2013). Therefore, it is apparent that additional regulatory mechanisms are also important to control Rca activity.

Rca *α* and β isoforms, which differ in ADP sensitivity, can be produced by both alternate splicing (Werneke et al., 1989; Rundle & Zielinski, 1991; To et al., 1999) or from transcription of independent genes (Rundle & Zielinski, 1991; Salvucci et al., 2003). In addition, the relative expression level and catalytic properties of Rca-α and Rca-β differ across species (Rundle & Zielinski, 1991; Crafts-Brandner et al., 1997; Carmo-Silva & Salvucci, 2013; Shivhare & Mueller-Cajar, 2017; Degen et al., 2021) and can be impacted by environmental factors such as temperature (Shivhare & Mueller-Cajar, 2017; Scafaro et al., 2019; Kim et al., 2020, 2021; Degen et al., 2021) to modulate CO_2 fixation under variable conditions.

Post-translational modification of Rca has also been proposed to provide an additional layer of regulation (Amaral et al., 2024). In Arabidopsis, Threonine 78 (Thr78) is phosphorylated in the dark and

under low light intensities, but not under high light, suggesting a regulatory role (Reiland *et al.*, 2009; Boex□Fontvieille *et al.*, 2014; Kim *et al.*, 2016). Functional support for this hypothesis came from several findings: (1) phosphorylation at Thr78 (Thr78-Rca) in Arabidopsis is reported to cause a significant decrease in plant biomass, due to a decreased Rubisco activation state (Kim *et al.*, 2019); (2) transgenic Arabidopsis plants expressing phospho-null mutants of Rca (T78A) had enhanced photosynthetic efficiency and plant growth; and (3) substitution of Thr78-to-Ser (T78S) resulted in hyper-phosphorylation, leading to reduced carbon assimilation and slower growth (Kim *et al.*, 2019). cpCK2 was shown to be the major kinase responsible for dark phosphorylation of AtRca, with loss-of-function mutant lines showing a reduction in Rca phosphorylation (Kim *et al.*, 2016). However, the phosphatase responsible for dephosphorylating Rca in the light has not been identified, and it is not clear whether this proposed mechanism is relevant outside of Arabidopsis. To address these issues, we sought to define the mechanisms controlling Thr78 phosphorylation, and prevalence of this post-translational modification in photosynthetic organisms. This was achieved by considering the following five questions, (1) what is the enzyme response for dephosphorylation of Thr78? (2) at what stage of flowering plant evolution did Thr78 emerge? (3) how conserved is Thr78 among photosynthetic angiosperms? (4) to what extent is Thr78 phosphorylated in different species? (5) and is light-dependent de-phosphorylation of Thr78 a general mechanism of controlling of RCA activity?

MATERIAL AND METHODS

Determination of Rca isoform and photosynthetic species containing Thr78-Rca

To analyze the conservation of Thr78 in Rca protein across plant species, the sequence of Arabidopsis Rca (AtRca: AT2G39730) was retrieved from the *Arabidopsis thaliana* TAIR10 genome assembly (Lamesch *et al.*, 2012) on Phytozome v13 (Goodstein *et al.*, 2012). Syntelogs to AtRca (i.e., shared positional homology along chromosomes) were subsequently identified in monocots (*Setaria viridis* Rca: Sevir.8G261433) and asterids (*Mimulus guttatus* Rca: Migut.F00758), which have homology to this sequence using either synteny mapping features on CoGe (Lyons & Freeling, 2008; Lyons *et al.*, 2008). Setaria Rca was chosen as an example of a gene that has been previously characterized (Kim et al., 2021) while Mimulus shares comparable synteny to Arabidopsis in the genomic region surrounding Rca enabling identification of syntelogs in the asterids. Working from these three representatives, additional syntelogues were locally identified based on their closest known Rca sister lineage within the Angiosperm phylogeny across other accessible plant genomes on these databases. *Amborella trichopoda* was leveraged as an outgroup for flowering plants in this case study given that this is known to be the one of the earliest diverging lineages for flowering plants (Soltis *et al.*, 2011). Additionally, homologues were surveyed, which contained threonine at position 78 phosphorylation site even if they didn't precisely fit

this stringent criterion of synteny using pBLAST on NCBI (https://blast.ncbi.nlm.nih.gov/Blast.cgi) for key agronomic model systems. This ultimately resulted in 217 isoform CDS sequences being identified. Alternative splicing of the same locus in some lineages meant that these CDS sequences represented 153 unique genes from across 91 species and 50 plant families. The longer, Rca-α, sequence was preferentially retained as a taxonomic representative for each alternative splicing gene when available for phylogenetic analysis. The CDS sequence of these genes were visualized in Seaview (Gouy *et al.*, 2010) and codon-aligned using MUSCLE (Edgar, 2004). Obvious pseudogenes that were missing large portions of their AAA+ ATPase domain such as the rice sequence (LOC_Os11g47980) were removed prior to phylogenetic analysis of this DNA alignment. A maximum likelihood tree was subsequently assembled using IQTree (Nguyen *et al.*, 2015) with the Amborella Rca sequence being specified as an outgroup and 1000 bootstraps being run to generate statistical support for nodes along the tree with the automatic substitution model selection determining a SYM+R8 model was the best-fit according to Bayesian Information Criterion. The resulting treefile was then visualized either in Figtree (http://tree.bio.ed.ac.uk/software/figtree/) (Figure S3) or in R using the Phytools and Ape libraries (Paradis & Schliep, 2019; Revell, 2024). Ancestral state reconstructions were performed using the Ape function *ace* particularly for the original position 78 amino acid identity between syntelogous genes, and the manner of α/ß origin (either by alternative splicing or distinct genes) for each plant family (Figure S4).

Plant growth and stress treatment

Arabidopsis Col-0 and camelina seeds were sterilized in 1 % (v/v) bleach for 5 min, rinsed with 70 % EtOH, and dried on filter paper. The sterilized seeds were sown on MS (Murashige and Skoog basal salt mixture powder, Phyto Technology Laboratories, M524) agar (0.8 %, w/v, Sigma-Aldrich, A1296) with 1 % (w/v) sucrose. The plates were stored at 4 °C for 2 days for cold stratification before transfer to a growth chamber. Seedlings were transferred into pots (5 cm diameter) filled with soil (Berger; PRO-MIX BX All Purpose Growing Mix) before the third true leaf emerged, which was approximately 5 to 7 days after germination (DAG). The other plants (brassica, soybean, green bean, and Medicago) were directly sown in soil after sterilization. Arabidopsis homozygous mutants of SLP1 (SALK_129247C) were ordered from ABRC, and homozygous lines were confirmed by genomic DNA PCR using LB_6313R (TCAAACAGGATTTTCGCCTGCT), SLP1_LP (GCCTGATCATCAAGTGACCTC) and SLP1_RP (CGGGAACCATGTCTGACTTAG) xfs designed using iSect tool by SALK (http://signal.salk.edu/tdnaprimers.2.html) (Alonso *et al.*, 2003). All plant species were grown at 22 °C, 16 h light and 8 h dark, 200 µmol m^{-2} s^{-1} PPFD with 2100 K 400W high pressure sodium bulbs (Ceramalux ALTO; C400S51).

Protein extraction and immunoblotting assay

Total proteins were extracted from three frozen leaf discs (1 cm in diameter) using a Qiagen Tissuelyzer for tissue grinding. The ground tissue was suspended in 0.5 mL of extraction buffer containing 62.5 mM Tris-HCl (pH 6.8), 2% SDS, 10% glycerol, 0.35 M 2-mercaptoethanol, and 0.001% protease inhibitor cocktail (Sigma-Aldrich; P9599). The suspension was heated at 95°C for 5 minutes to denature proteins and inactivate proteases, followed by centrifugation at 13,500 rpm for 30 minutes at 4°C. The supernatant was collected, and 10 µL aliquots were separated on 10% SDS-PAGE gels. Proteins from the gels were transferred electrophoretically to 0.2 µm nitrocellulose membranes (Bio-Rad) and blocked with PBS solution with 5% (w/v) non-fat milk powder (Sigma) for 1h at room temperature. For immunodetection, primary antibodies were diluted in Intercept Blocking Buffer (LI-COR; 927-70001); anti-Rca (Agrisera; AS10 700) at 1:5000 and anti-pT78 (GenScript) at 1:4000, and incubated overnight at 4°C. Modification-specific antibody was generated against the phosphopeptide antigen RGLAYDpT78DDQQDC (Arabidopsis anti-pT78). For each peptide antigen, the Cys residue at the N- or C-terminus was added for coupling to keyhole limpet hemocyanin (KLH). All custom antibodies were produced by GenScript (Piscataway, NJ, USA). Secondary detection used a fluorescent goat anti-rabbit antibody (Invitrogen; A32735) at a 1:10,000 dilution in PBS-T, incubated for 1 h at room temperature, and visualized with a LI-COR Odyssey Infrared Imaging System. All immunoblotting experiments were conducted at least twice to ensure reproducibility of results.

Protein phosphorylation assay with phosphatase inhibitor

WT Col-0 plants were grown as described above and whole rosettes were sampled and dipped in the protein phosphatase inhibitor buffer: 1% (v/v) solution of phosphatase inhibitor cocktail 2 (Sigma: P5726) and phosphatase inhibitor cocktail 3 (Sigma: P0044), overnight under dark. For dark treatment samples, the protein extraction was done using the overnight incubated samples and for light treatment samples the rosettes were exposed to 150 µmol m^{-2} s^{-1} PPFD light for 2 h and then total protein was extracted.

Physiological analysis

For light induction analysis, the leaves of 5-week WT and *slp1* mutants were dark adapted overnight before measurement in a portable infra-red gas exchange system (LI-6800, LICOR Environmental, Lincoln, Nebraska, USA) connected to a multiphase flash fluorometer (6800-01A) with a 2 cm^2 chamber. During low light incubation the plants were managed under dark conditions to make sure that Rca remained phosphorylated in both WT and *slp1* mutants. The chamber settings were 1:1 red:blue

ratio, leaf temperature of 22 °C, CO_2 level of 420 µmol mol^{-1}, and 50% relative humidity. The measurement started with a low light of 20 µmol m^{-2} s^{-1} photosynthetic photon flux density (PPFD) for 20 min, then the PPFD was increased to high light conditions of 1000 µmol m^{-2} s^{-1} for 60 min, measurements were logged every 10 s. For CO_2 response analysis, plants were measured at the same high light conditions described above after finishing the light induction measurement. The CO_2 level was adjusted to produce a plot of net CO_2 assimilation against intercellular CO_2 concentration (A-C_i curve). The CO_2 levels were changed every 90 – 120 s in the following order: 420, 300, 200, 100, 50, 10, 420, 420, 420, 600, 800, 1200, 1800 µmol mol^{-1}. The relative comparisons and significant differences between *slp1* and WT were determined using students t-test (n = 4 to 6).

Statistical Analysis

Comparisons of rosette size and assimilation rate between *slp1* and WT were done using a two-tailed Students' t-test using data from four to six biological replicates (individual plants) in Microsoft Excel v16.88.

RESULTS

SHEWENELLA-LIKE PROTEIN PHOSPHATASE 1 (SLP1) dephosphorylates Rca in-vivo

Light-dependent dephosphorylation of AtRca suggested that an unknown protein phosphatase is operating. To test this hypothesis, the phosphorylation state of Rca was assessed under light and dark conditions in the presence and absence of a protein phosphatase inhibitor cocktail (PPIC) (Fig. 1A and B). Under dark conditions, Rca phosphorylation increased compared to the sample lacking PPIC (Fig. 1B) which is consistent with the presence of a protein phosphatase. Dephosphorylation of Rca occurred in the light (Fig. 1B), even in the presence of the PPIC, which may be because the level of dephosphorylation exceeded the ability of the PPIC to inhibit activity. To identify the gene responsible for dephosphorylation of Rca, all known chloroplast localized protein phosphatases in Arabidopsis (White-Gloria *et al.*, 2018) were screened for reported associations with Rca in the literature and co-expression databases. Out of 9 chloroplast localized protein phosphatases, AtSLP1 (AT1G07010) showed a potential association based on co-expression (Fig. 1C). We hypothesized that in the absence of *AtSLP1*, AtRca will not be dephosphorylated in the light. To test this, a homozygous T-DNA insertion mutant of *slp1* was identified (Figure S1) and assessed for the ability to dephosphorylate Rca in the dark and light. *slp1* mutants showed phosphorylation of Rca in the dark, as also observed in the case of Col-0, but in the mutant phosphorylation was observed to persist in the light (Fig. 1D).

We hypothesized that lack of Rca dephosphorylation in *slp1* mutants would lead to decreased photosynthesis and a growth penalty. Analysis of 5-week-old plants found *slp1* mutants have a significant

reduction in rosette size relative to Col-0 under normal light conditions (Fig. 1E and F). To assess the impact of SLP1 on steady state photosynthesis, A/Ci (net CO_2 assimilation vs internal CO_2 concentration) curves were performed on Col-0 and *slp1* mutants, finding no difference between lines (p=0.05; Figure S2). As there is a tight correlation between Rubisco activation state and the rate of induction of photosynthesis during shade to sun transitions, the impact of SLP1 on the rate of photosynthetic induction after a step-increase in photosynthetic photon flux density from 20 to 1000 µmol m^{-2} s^{-1} was assessed, again finding no significant difference compared to Col-0 (p=0.05; Fig. 1G).

Thr 78 in Rca is common

To study the conservation of Thr78 (Arabidopsis numbering) in Rca, 1893 protein sequences from 479 plants species were assessed. Among these, 203 species retained Thr78 (Table S1). Next, a more stringent synteny informed ortholog phylogeny of Rca-α and Rca-β isoforms was generated across angiosperms to address the questions: at what stage of flowering plant evolution did the putative Thr78 phosphosite emerge, and how well conserved is it among photosynthetic angiosperms? Leveraging maximum likelihood gene family phylogeny ancestral states, Thr78 distribution was estimated for each family, including deeper nodes within the tree such as the branch point of the *Amborellaceae* (Fig. 2). The presence of Thr78 was observed in most plant families (Fig. 2), while among the *Poaceae*, that includes major crop species, the presence of Isoleucine (Ile) was found to dominate at position 78 compared to Threonine (Fig. 2). The difference in the abundance of both amino acids, Thr and Ile at this site is similar at the evolutionary scale, and an estimate of the ancestral state was ambiguous. Interestingly, the *α* and *β* copies appeared polyphyletic, with multiple origins of the two isoforms arising from alternate splicing or gene duplication across the phylogeny (Fig. S4, and S5). Within the Brassicaceae *Arabidopsis thaliana* and its immediate relatives all appear to have a single copy of Rca with alpha and beta forms being the result of alternative splicing of a single transcript.

By contrast in the Fabaceae, *Glycine max* has four gene copies of Rca (two each of *α* and *β*) with the Papillionoid legumes more generally having two copies of Rca. There is no equivalent duplication event in *Cercis canadensis* that would indicate a Fabaceae-wide pattern. Therefore, this pattern of two Papillionoid copies is consistent with the whole-genome doubling (WGD) event preceding the diversification of this subfamily, and by undergoing an additional allopolyploid event, *Glycine max* has two additional copies for each of these ancestral homeologues (Gill, *et al.*, 2009; Koenen, *et al.*, 2021). Within Poaceae, *Setaria viridis* and the grasses more generally displayed two mirrored clades, which reflect the known taxonomic sorting of this family. The grass family has undergone three WGD events (τ, σ, and ρ), two of which are shared with monocots, with the p WGD unique to the Poaceae (Paterson *et al.*, 2004; Tang *et al.*, 2010; McKain *et al.*, 2016). Although superficially resembling the *ρ* WGD event, these

grass copies are physically proximal to their sister copies in the adjacent clade suggesting that this may instead be an ancient tandem duplication event.

Light-dependent dephosphorylation of Thr78 in Rca is unique to Arabidopsis

Previous reports showed that both AtRca isoforms phosphorylate in the dark and are dephosphorylated as plants are exposed to light. To test whether Thr78 phosphorylation status is light-sensitive in species other than Arabidopsis, we screened three C3 plants from the *Brassicaceae* for dark-dependent phosphorylation of Thr78, using a pT78 antibody (Kim et al., 2019) (Fig. 3A). As in Arabidopsis, Rca-α and Rca-β isoforms arise from alternate splicing in *Brassicaceae* and the Thr78 site is conserved in all proteins (Fig. 3B). However, unlike Arabidopsis, Rca in *Camelina sativa* (*Cs*), *Brassica oleraceae* (*Bo*) and *Brassica napus* (*Bn*) phosphorylated in dark but lacked light-induced dephosphorylation (Fig. 3A). These data suggest that although Thr78 is phosphorylated in multiple species, light-dependent regulation may be specific to Arabidopsis.

To broaden the analysis, we performed the dephosphorylation assay on several legumes: *Glycine max* (*Gm*), *Phaseolus vulgaris* (*Pv*), and *Medicago truncatula* (*Mt*). The Rca isoforms in these species are derived from individual genes of *Rca-α* and *Rca-β*, unlike the situation in the *Brassicaceae*. The Rca-α isoforms retain Thr78, whereas the β isoforms have Ile78 in *Gm* and *Mt*, and Val78 in *Pv* (Fig. 3B). Publicly available data suggest the transcription level of Rca-α is low relative to β in both *Gm* and *Pv*, and moderately expressed in *Mt* (Table S2). The light/dark assay on legume plants showed that both the isoforms were expressed, and phosphorylated in the dark, but as with the Brassicaceae, did not dephosphorylate in the light (Fig. 3A). The reason why the antibody was able to detect phosphorylation of β forms, which lack Thr78, is unclear. It is possible that there is relaxed selectively, but we consider these results with caution.

To study the impact of phosphorylation in C4 grass plants, we analyzed Rca phosphorylation in four species of C4 grass: *Sorghum bicolor* (*Sb*), *Miscanthus* (*Ms*), *Saccharum officinarum* (*Su*), and *Setaria viridis* (*Sv*) (Fig. 4A). Each of these species possess two separate genes for the alternative Rca isoforms, with Rca-α containing Thr78, but with it lacking from Rca-β (Fig. 4B, C). In accordance with previous reports (Kim *et al.*, 2021), only the Rca-β isoform could be detected under normal growth conditions (Fig. 4A and C). An unspecific cross-reaction was present in C4 grass samples probed with pT78 antibody, but the detected protein was too large to be Rca-β, subsequently no phosphorylation of Rca-β was detected (Fig. 4A). To test whether a C4 Rca-α isoform could be phosphorylated, sorghum plants were exposed to heat induce Rca-α isoform expression (Fig. 4C). Plants accumulated SbRca-α after 24 h heat treatment, but no bands of the correct size could be detected using the pT78 antibody (Fig.

4C). To rule out the possibility that a lack of detectable Thr78 phosphorylation was due to high protein phosphatase activity, the assay was repeated in the presence of a protein phosphatase inhibitor cocktail (PPIC), but again protein phosphorylation was not observed under any condition (Fig. 5). This result suggests that SbRca-α T78 is not phosphorylated by cpCK2 as it is in Arabidopsis even though the gene for cpCK2 is present in sorghum.

DISCUSSION

Rca is subject to multiple levels of regulation to adjust carbon fixation in response to environmental conditions (Amaral *et al.*, 2024). Differences in gene expression, biochemical properties of isoforms, redox status, and post-translational modification of Rca have been topics of investigation (Boex□Fontvieille *et al.*, 2014; Kim *et al.*, 2016, 2019). Dark dependent phosphorylation of Thr78 is proposed to downregulate Rca activity leading to reduced assimilation (Kim et al. 2019). cpCK2 is described as the major kinase responsible for phosphorylation of AtRca Thr78 based on dramatically reduced phosphorylation in *cpcpk2* T-DNA insertion lines (Kim *et al.*, 2016). Here we identified Shewanella-like protein phosphatase 1 (SLP1) as the second component of this regulatory mechanism, acting to dephosphorylate AtRca Thr78 in the light (Fig. 1). SLP1 is a highly conserved protein phosphatase reported to be blue light responsive in Arabidopsis (Depuydt & Vandepoele, 2021) and belongs to a protein family consisting of two members, of which, SLP1 is the only chloroplast localized isoform (Uhrig & Moorhead, 2011). A role for mitochondrial targeted SLP2 has been described in negative regulation of gibberellic acid related seed germination (Uhrig *et al.*, 2017), but the physiological role and targets of SLP1 have not previously been reported.

If phosphorylation of Rca has a dominant impact on activity, plants lacking SLP1 would be predicted to see an increase Thr78 phosphorylation in the light, leading to lower Rubisco activity, and lower A_{net}, an impact on photosynthesis, with no difference observed in assimilation rates between WT and knockout lines during light induction or CO_2 response (Fig. 1G and Fig. S2). These findings are in keeping with observations by Kim *et al.* (2016), who reported no change in assimilation rates when Thr78 phosphorylation state was reduced in *cpck2* mutants. These results were attributed to redundancy in Rca regulation between protein phosphorylation and control by thioredoxin (Kim *et al.*, 2016) and the same rationale may apply here. Support for a functional role for phosphorylation of Thr78 in Arabidopsis has only been shown in Rca variant lines lacking the redox sensitive C-terminal extension (Kim *et al.*, 2019). Our analysis, conducted on lines containing the C-terminal extension, are therefore consistent with the hypothesis that Rca possesses multiple redundant regulatory mechanisms in Arabidopsis, which operate to regulate activity in response to variable light environments. The impact of SLP1 on photosynthesis may only be apparent in the absence of redox regulation.

Despite the absence of impact on A_{net}, the *slp1* mutant showed reduced growth (Fig. 1). Given that the *cpck2* mutant, which also showed altered phosphorylation of Rca, did not have a growth phenotype, we attribute this to an unrelated impact on chloroplast physiology. As a largely uncharacterized protein, the specificity and targets of SLP1 are unknown. Phosphatases have traditionally been considered promiscuous, with specificity dictated by regulatory subunits (Virshup and Shenolikar, 2009). SLP1 is not known to have regulatory subunits, it is therefore conceivable there are other targets within the chloroplast that are impacted in the mutant leading to the observed growth phenotype.

Substitution of Thr78 with Serine lead to a relative increase in phosphorylation at the site, in Arabidopsis resulted in smaller plants with decreased photosynthesis (Kim *et al.*, 2019). Altering a single amino acid, Thr78, was proposed as a means of generating plants with better photosynthesis. However, the prevalence of Thr78 across species, the frequency of post-translational modification and functionality were unclear. To begin to address these questions we expanded previous searches of genomic databases, which assessed the evolution of Rca copy number across the green lineage (Nagarajan & Gill, 2018; Kim *et al.*, 2019), to use a synteny based approach. Nagarajan and Gill (2018) placed the emergence of the Rca-α CTE and alternate splicing mechanisms in the charophytes, before the divergence of land plants and there is only one reported example of a species only having evidence for expression of Rca α (Nagarajan & Gill, 2018). Here, despite α and β forms (bearing or lacking a c-terminus respectively) occurring within each model system, these α and β forms appear to represent repeated cases of evolutionary convergence on these two isoforms (Fig S5) through distinct means within each clade: subfunctionalization (Birchler & Yang, 2022), following tandem duplication in the grasses as previously described (Nagarajan & Gill, 2018), WGD in the legumes, or alternative splicing of a single coding sequence into alternative isoforms in Brassicaceae. This may suggest that Rca isoforms can be quite plastic in the way they arise within distinct plant families where α and β forms may not necessarily reflect true homology within Rubisco activase isoforms.

Previous assessment of a smaller number of Rca sequences failed to identify any with Thr78 replaced by Serine, leading to speculation that the configuration with the attendant hyper phosphorylation observed in Arabidopsis has been selected against (Kim *et al.*, 2019). In the initial set of Rca sequences identified by BLAST search, we identified gene models from at least seven species (Table S1) which do have Ser78, although these were not considered orthologs in the synteny analysis. Of the 25 species found to contain Rca sequences with Thr78, it remains to be seen how many undergo phosphorylation. Our data are consistent with it occurring in at least the Brassicaceae, while phosphorylation of an equivalent Thr residue has been reported in tomato, suggesting this modification may occur more widely (Marques et al., 2021).

We found no evidence for phosphorylation of Thr78 in monocot species, including Sorghum, Setaria, sugarcane and Miscanthus. The peptide fragment used for antibody generation is highly conserved, with 100% identity between Arabidopsis Rca and Sorghum Rca-α "RGLAYDTSDDQQDC" and should therefore have been able to detect phosphorylation if present under the conditions tested. There are several potential explanations for this finding, including an absence of the kinase, differences in localization or expression profiles of the kinase, or regulation of the kinase. In Arabidopsis, Rca is phosphorylated by cpCK2 (Kim et al., 2016). A homologous gene has been characterized in rice (LOC_Os03g55490) (Lu et al., 2015) and syntenic sequences can be found in C4 grasses including Sorghum (Sobic.001G07970) (Carvalho et al., 2020). As Sorghum operates two-celled C4 photosynthesis for an interaction to occur between Rca and cpCK2 both must be expressed in the same cell type. Transcriptomics suggests that cpCK2 is expressed in both mesophyll and bundle sheath cells in maize (Chang et al., 2012), Setaria (John et al., 2014) and Sorghum (Döring et al., 2016), albeit with ~2-fold mesophyll enrichment in maize and Setaria whereas Rca is localized in the bundle sheath. Even so, it appears that the orthologous cpCK2 is present in the same compartment as Rca (i.e., the bundle sheath cell chloroplast). However, in the monocot species tested Rca-β, which lacks Thr78, is the predominate isoform under normal conditions and Rca-α, which possess Thr78, is induced during stress (Shivhare & Mueller-Cajar, 2017; Scafaro et al., 2019; Kim et al., 2020, 2021). Whether C4 monocot cpCK2 retains the ability to phosphorylate Thr78 in Rca-α, or if the bundle sheath stromal environment is permissive for phosphorylation remains unclear (Kim et al., 2016). CK2 exists as a multigene family, composed of catalytic α subunits and regulatory beta subunits (Salinas et al., 2006; Schweer et al., 2010), which form hetero-tetramers that can differ in substrate specificity (Domańska et al., 2005). Intriguingly there appears to be a lack of regulatory β subunits in the chloroplast (Salinas et al., 2006), so differences in regulatory subunits impacting specificity appears unlikely, although multiple chloroplast CK2 containing complexes have been detected (Baginsky et al., 1997) suggesting the protein does not act alone. However, further research is required to characterize the regulation of monocot cpCK2 and whether it can phosphorylate Rca.

Conservation of phosphorylation of Thr78 in some C3 plants is not evidence of a conserved regulatory role. Indeed, in the species examined, strong evidence for light-dependent dephosphorylation of Thr78 was only found for Arabidopsis, with phosphorylation of Rca detected in both the light and dark in other C3 species (Fig. 3). These data may suggest a limited scope for phosphorylation as a means of regulation, with most species depending on other mechanisms, such as changes in redox state, catalytic properties or expression. It may be that alternate post-translational modifications of Rca have greater importance in other species and several different ones have been described (Amaral et al., 2024). Interestingly, there are several reports of phosphorylation of S79 in Arabidopsis (Willems et al., 2019),

and this modification was also observed in a Brachypodium, Chlamydomonas and maize (Willems et al., 2019, 2024). Further phosphoproteomics of maize during a diurnal cycle suggests that rather than Thr78, Ser79 undergoes dark-dependent phosphorylation (Gao et al., 2023). However, the prevalence of S79 phosphorylation is also likely to vary, as seen by a failure to detected in protein samples from *Glycine max* (soybean-S86) (Soleh et al., 2017) .Therefore, the prevalence and function of Ser79 phosphorylation is unclear, and whether it can play a similar role to Thr78 warrants further investigation.

Taken together our results suggest that Thr78 can be found in Rca sequences across the green lineage, although the prevalence varies, and degree to which it undergoes phosphorylation is inconsistent. Our data provides support for a mechanism whereby Thr78 is phosphorylated in the dark by cpCK2 and dephosphorylated in the light by SLP1 in Arabidopsis. The lack of impact on photosynthesis when cpCK2 or SLP1 are knocked out suggest that phosphorylation of Thr78 acts redundantly with redox regulation. More widely, it is likely that regulation of Rca can occur through multiple mechanisms, including redox, sensitivity to ADP and gene expression and the relative importance of each varies.

Acknowledgments

We would like to thank Toby Kellogg and Shawn Abrahams for providing feedback on the phylogenic analyses. This work was funded by the DOE Center for Advanced Bioenergy and Bioproducts Innovation (U.S. Department of Energy, Office of Science, Biological and Environmental Research Program under Award Number DE-SC0018420). Any opinions, findings, and conclusions or recommendations expressed in this publication are those of the author(s) and do not necessarily reflect the views of the U.S. Department of Energy.

Competing interests

The authors report no conflict of interest

Authors contributions

Conceptualization (SK, NB, SJB, DO), Investigation (NB, SC, MS, JH, SK), Formal Analysis (NB), Project administration (NB, SJB, DO), Supervision (AL, SJB, DO), Visualization (NB), Writing - original draft (NB, JH, SC, DO, SJB), Writing – review and editing (NB, JH, DO, AL, SJB).

FIGURE LEGENDS

Figure 1: SLP1 dephosphorylates Rca in Arabidopsis. Protein phosphatase assay with PPIC (+P) and without PPIC (-P) isoforms, comparing total abundance (A) to phosphorylation (B) of Rca by immunoblot. (C) Putative protein-protein interactions between Rca and chloroplast localized protein phosphatases. (D) Immunoblot analysis of light dependent dephosphorylation of Rca in WT (Col-0) and *slp1* mutants. (E) Image of 5-week-old rosettes comparing WT (Col-0) and slp1 plants. (F) Comparison of rosette size between WT (Col-0) and slp1 plants (n=20). (G) Photosynthetic induction curves of WT (Col-0) and *slp1* mutant plants (n=5 to 6).

Figure 2: Phylogenetic representation of the amino acid present at the phosphorylation site (peptide position 78) within extant Rca gene models. Ancestral states for families, and when available deeper orders of Angiosperms, are denoted at their corresponding nodes as pie charts. The nodes depicting the presence of Thr78 is colored green and the ones with Ile78 is colored navy blue. Less abundant amino acids at the peptide position 78 are depicted as varying shades of blue and purple. The detailed confirmation of bootstrap values is mentioned in Figure S3.

Figure 3: Light dependent dephosphorylation of Thr78 in Rca is specific to Arabidopsis. (A) Immunoblot analysis comparing protein phosphorylation and total abundance of Rca under light (L) and dark (D) conditions (At: *Arabidopsis thaliana*, Cs: *Camelina sativa*, Bn: *Brassica napus*, Bo: *Brassica oleraceae*, Gm: *Glycine max*, Pv: *Phaseolus vulgaris*, Mt: *Medicago truncatula*). The upper panel shows the total Rca protein extracted from plant samples and the middle panel shows the phosphorylated Rca protein. α and β denote the 2 isoforms of Rca protein. CBB (Coomassie Brilliant Blue) depicts the loading control. (B) Sequence alignment depicting the conservation of Thr78 amino acid in C3 species. The amino acid lacking color codes depicts the change in the Thr78 site to Isoleucine (*I*) in *Glycine max* and *Medicago truncatula*, and Valine (*V*) in Phaseolus vulgaris. The letter "A" and "B" at the end of the species labelling denotes the Rca-α and Rca-β isoforms. (C) The phylogenetic tree depicts the division of C3 Brassicaceae family and legumes based on Rca isoforms arising from protein splicing in Brassicaceae as compared to different genes in legumes and presence and absence of Thr78 amino acid in the Rca-β isoform. The blue boxes depict the presence of Thr78 amino acid whereas the red depicts the lack of Thr78. The yellow box depicts the experimental confirmation of protein phosphorylation at Thr78 phosphosite.

Figure 4: Phosphorylation of Rca is not observed in selected C4 moncots. (A) Protein phosphorylation assay depicting four C4 plant samples in light and dark conditions (At: *Arabidopsis thaliana*, Sv: *Setaria viridis*, Sb: *Sorghum bicolor*, Su: *Saccharum officinarum*, Ms: *Miscanthus*). The upper panel shows the accumulation of Rca protein quantified with Anti-Rca antibody and middle panel shows the

phosphorylated Rca protein quantified with Anti-pT78 antibody. α and β denote the 2 isoforms of Rca protein. CBB denotes the loading control. (B) Sequence alignment of motif comparing Arabidopsis and select C4 plants. (C) Immunoblot analysis comparing Rca phosphorylation under heat for 24 h in WT sorghum. The numbers denote the time in hours after the heat stress. CBB denotes the loading control.

Figure 5: Sorghum lacks phosphorylation of Thr78 with or without PPIC treatment. (A) Immunoblot analysis comparing sorghum WT samples collected after heat stress at 42°C under light and dark treatment. The control samples were collected at 28°C. The + and – sign denotes presence and absence of treatment, respectively. The left panel shows Rca protein accumulation and right panel depicts analysis using anti-pT78 antibody.

Figure S1: The genomic DNA (gDNA) PCR with primer combinations of LB, LP and RP showed that LB primer T-DNA insertion was confirmed in homozygous lines whereas WT showed no bands (upper panel). The SLP1 gene primers showed gDNA bands in the WT and not in the *slp1* mutants (lower panel).

Figure S2: The *ACi* curve showed that both WT (Col-0) and slp1 mutants overlap suggesting that both the genotypes have no difference in the photosynthetic efficiency. Error bars denote standard error. Green dots are *slp1* mutants and black dots are WT (Col-0).

Figure S3: The conservative phylogeny structure of Rca orthologs where all nodes with bootstrap support (blue numbers) greater than 80% being retained whereas other lower support nodes were collapsed into polytomies.

Figure S4: Rca α (white) and β (black) isoforms on extant gene models as well as alternatively spliced gene models which produce both Rca α and β (grey). Ancestral states for families, and when available deeper orders of Angiosperms, are denoted at their corresponding nodes as pie charts.

Figure S5: The likely pattern that could result in the polytomies of α and β isoforms ancestry states that Angiosperms initially beginning as Rca α lineages out of which β isoforms repeatedly arise independently following either subfunctionalization of duplicate gene copies or alternative splicing of α gene models to β isoforms as well. Within certain lineages where α isoforms are lost all the Rca copies become canalized into a β isoform state thereafter.

Table S1: List of Rca protein sequences identified by BLAST search.

Table S2: Relative expression and residue at site equivalent to AtRca T78 for Rca isoforms from *G. max*, *M. truncatula* and *P. vulgaris.*

REFERENCES

Alonso JM, Stepanova AN, Leisse TJ, Kim CJ, Chen H, Shinn P, Stevenson DK, Zimmerman J, Barajas P, Cheuk R, *et al.* 2003. Genome-wide insertional mutagenesis of Arabidopsis thaliana. *Science (New York, N.Y.)* **301**: 653–7.

Amaral J, Lobo AKM, Carmo□Silva E. **2024**. Regulation of Rubisco activity in crops. *New Phytologist* **241**: 35–51.

Baginsky S, Tiller K, Link G. **1997**. Transcription factor phosphorylation by a protein kinase associated with chloroplast RNA polymerase from mustard (Sinapis alba). *Plant Molecular Biology* **34**: 181–189.

Birchler JA, Yang H. **2022**. The multiple fates of gene duplications: Deletion, hypofunctionalization, subfunctionalization, neofunctionalization, dosage balance constraints, and neutral variation. *The Plant Cell* **34**: 2466–2474.

Boex□Fontvieille E, Daventure M, Jossier M, Hodges M, Zivy M, Tcherkez G. **2014**. Phosphorylation pattern of <scp>R</scp> ubisco activase in *<scp>A</scp> rabidopsis* leaves. *Plant Biology* **16**: 550–557.

Carmo-Silva AE, Salvucci ME. **2013**. The Regulatory Properties of Rubisco Activase Differ among Species and Affect Photosynthetic Induction during Light Transitions . *Plant Physiology* **161**: 1645–1655.

Carvalho DS, Nishimwe A V., Schnable JC. **2020**. IsoSeq transcriptome assembly of C_3 panicoid grasses provides tools to study evolutionary change in the Panicoideae. *Plant Direct* **4**.

Chang Y-M, Liu W-Y, Shih AC-C, Shen M-N, Lu C-H, Lu M-YJ, Yang H-W, Wang T-Y, Chen SC-C, Chen SM, *et al.* 2012. Characterizing Regulatory and Functional Differentiation between Maize Mesophyll and Bundle Sheath Cells by Transcriptomic Analysis . *Plant Physiology* **160**: 165–177.

Crafts-Brandner SJ, van de Loo FJ, Salvucci ME. **1997**. The Two Forms of Ribulose-1,5-Bisphosphate Carboxylase/Oxygenase Activase Differ in Sensitivity to Elevated Temperature. *Plant Physiology* **114**: 439–444.

Crafts-Brandner SJ, Salvucci ME. **2002**. Sensitivity of Photosynthesis in a C4 Plant, Maize, to Heat Stress. *Plant Physiology* **129**: 1773–1780.

Degen GE, Orr DJ, Carmo□Silva E. **2021**. Heat□induced changes in the abundance of wheat Rubisco activase isoforms. *New Phytologist* **229**: 1298–1311.

Depuydt T, Vandepoele K. **2021**. Multi□omics network□based functional annotation of unknown Arabidopsis genes. *The Plant Journal* **108**: 1193–1212.

Domańska K, Zieliński R, Kubiński K, Sajnaga E, Masłyk M, Bretner M, Szyszka R. **2005**. Different properties of four molecular forms of protein kinase CK2 from Saccharomyces cerevisiae. *Acta biochimica Polonica* **52**: 947–51.

Döring F, Streubel M, Bräutigam A, Gowik U. **2016**. Most photorespiratory genes are preferentially expressed in the bundle sheath cells of the C_4 grass *Sorghum bicolor*. *Journal of Experimental Botany* **67**: 3053–3064.

Flecken M, Wang H, Popilka L, Hartl FU, Bracher A, Hayer-Hartl M. **2020**. Dual Functions of a Rubisco Activase in Metabolic Repair and Recruitment to Carboxysomes. *Cell* **183**: 457-473.e20.

Gao Z, Yang X, Mei Y, Zhang J, Chao Q, Wang B. **2023**. A dynamic phosphoproteomic analysis provides insight into the <scp>C4</scp> plant maize (*Zea mays* L.) response to natural diurnal changes. *The Plant Journal* **113**: 291–307.

Goodstein DM, Shu S, Howson R, Neupane R, Hayes RD, Fazo J, Mitros T, Dirks W, Hellsten U, Putnam N, *et al.* 2012. Phytozome: a comparative platform for green plant genomics. *Nucleic Acids Research* **40**: D1178–D1186.

Gouy M, Guindon S, Gascuel O. **2010**. SeaView Version 4: A Multiplatform Graphical User Interface for Sequence Alignment and Phylogenetic Tree Building. *Molecular Biology and Evolution* **27**: 221–224.

Hudson GS, Evans JR, von Caemmerer S, Arvidsson YBC, Andrews TJ. **1992**. Reduction of Ribulose-1,5-Bisphosphate Carboxylase/Oxygenase Content by Antisense RNA Reduces Photosynthesis in Transgenic Tobacco Plants. *Plant Physiology* **98**: 294–302.

Jiang C, Quick WP, Alred R, Kliebenstein D, Rodermel SR. **1994**. Antisense RNA inhibition of Rubisco activase expression. *The Plant Journal* **5**: 787–798.

John CR, Smith-Unna RD, Woodfield H, Covshoff S, Hibberd JM. **2014**. Evolutionary Convergence of Cell-Specific Gene Expression in Independent Lineages of C4 Grasses . *Plant Physiology* **165**: 62–75.

Kim SY, Bender KW, Walker BJ, Zielinski RE, Spalding MH, Ort DR, Huber SC. **2016**. The plastid casein kinase 2 phosphorylates rubisco activase at the Thr-78 site but is not essential for regulation of rubisco activation state. *Frontiers in Plant Science* **7**.

Kim SY, Harvey CM, Giese J, Lassowskat I, Singh V, Singh V, Cavanagh AP, Cavanagh AP, Spalding MH, Finkemeier I, *et al.* 2019. In vivo evidence for a regulatory role of phosphorylation of Arabidopsis Rubisco activase at the Thr78 site. *Proceedings of the National Academy of Sciences of the United States of America*.

Kim SY, Slattery RA, Ort DR. **2021**. A role for differential Rubisco activase isoform expression in C_4 bioenergy grasses at high temperature. *GCB Bioenergy* **13**: 211–223.

Kim SY, Stessman DJ, Wright DA, Spalding MH, Huber SC, Ort DR. **2020**. Arabidopsis plants expressing only the redox-regulated Rca-α isoform have constrained photosynthesis and plant growth. *Plant Journal* **103**: 2250–2262.

Lamesch P, Berardini TZ, Li D, Swarbreck D, Wilks C, Sasidharan R, Muller R, Dreher K, Alexander DL, Garcia-Hernandez M, *et al.* 2012. The Arabidopsis Information Resource (TAIR): improved gene annotation and new tools. *Nucleic Acids Research* **40**: D1202–D1210.

Lu Q, Ding S, Reiland S, Rödiger A, Roschitzki B, Xue P, Gruissem W, Lu C, Baginsky S. **2015**. Identification and characterization of chloroplast casein kinase II from Oryza sativa (rice). *Journal of Experimental Botany* **66**: 175–187.

Lyons E, Freeling M. **2008**. How to usefully compare homologous plant genes and chromosomes as DNA sequences. *The Plant Journal* **53**: 661–673.

Lyons E, Pedersen B, Kane J, Alam M, Ming R, Tang H, Wang X, Bowers J, Paterson A, Lisch D, *et al.* 2008. Finding and Comparing Syntenic Regions among Arabidopsis and the Outgroups Papaya, Poplar, and Grape: CoGe with Rosids. *Plant Physiology* **148**: 1772–1781.

Marques DN, Stolze SC, Harzen A, Nogueira ML, Batagin-Piotto KD, Piotto FA, Mason C, Azevedo RA, Nakagami H. **2021**. Comparative phosphoproteomic analysis of tomato genotypes with contrasting cadmium tolerance. *Plant Cell Reports* **40**: 2001–2008.

McKain MR, Tang H, McNeal JR, Ayyampalayam S, Davis JI, dePamphilis CW, Givnish TJ, Pires JC, Stevenson DWm, Leebens-Mack JH. **2016**. A phylogenomic assessment of ancient polyploidy and genome evolution across the Poales. *Genome Biology and Evolution*: evw060.

Nagarajan R, Gill KS. **2018**. Evolution of Rubisco activase gene in plants. *Plant Molecular Biology* **96**: 69–87.

Neuwald AF, Aravind L, Spouge JL, Koonin E V. 1999. AAA $^{+}$□: A Class of Chaperone-Like ATPases Associated with the Assembly, Operation, and Disassembly of Protein Complexes. *Genome Research* **9**: 27–43.

Nguyen L-T, Schmidt HA, von Haeseler A, Minh BQ. **2015**. IQ-TREE: A Fast and Effective Stochastic Algorithm for Estimating Maximum-Likelihood Phylogenies. *Molecular Biology and Evolution* **32**: 268–274.

Orr DJ, Robijns AKJ, Baker CR, Niyogi KK, Carmo-Silva E. **2023**. Dynamics of Rubisco regulation by sugar phosphate derivatives and their phosphatases. *Journal of Experimental Botany* **74**: 581–590.

Parry MAJ, Andralojc PJ, Scales JC, Salvucci ME, Carmo-Silva AE, Alonso H, Whitney SM. **2013**. Rubisco activity and regulation as targets for crop improvement. *Journal of Experimental Botany* **64**: 717–730.

Paterson AH, Bowers JE, Chapman BA. **2004**. Ancient polyploidization predating divergence of the cereals, and its consequences for comparative genomics. *Proceedings of the National Academy of Sciences* **101**: 9903–9908.

Poolman MG, Fell DA, Thomas S. **2000**. Modelling photosynthesis and its control. *Journal of Experimental Botany* **51**: 319–328.

Portis AR, Jr. 2003. Rubisco activase - Rubisco's catalytic chaperone. *Photosynthesis Research* **75**: 11–27.

Portis AR, Li C, Wang D, Salvucci ME. **2007**. Regulation of Rubisco activase and its interaction with Rubisco. *Journal of Experimental Botany* **59**: 1597–1604.

Qu Y, Mueller-Cajar O, Yamori W. **2023**. Improving plant heat tolerance through modification of Rubisco activase in C3 plants to secure crop yield and food security in a future warming world. *Journal of Experimental Botany* **74**: 591–599.

Reiland S, Messerli G, Baerenfaller K, Gerrits B, Endler A, Grossmann J, Gruissem W, Baginsky S. **2009**. Large-Scale Arabidopsis Phosphoproteome Profiling Reveals Novel Chloroplast Kinase Substrates and Phosphorylation Networks . *Plant Physiology* **150**: 889–903.

Ristic Z, Momčilović I, Bukovnik U, Prasad PVV, Fu J, DeRidder BP, Elthon TE, Mladenov N. **2009**. Rubisco activase and wheat productivity under heat-stress conditions. *Journal of Experimental Botany* **60**: 4003–4014.

Robinson SP, Portis AR. **1989**. Adenosine triphosphate hydrolysis by purified rubisco activase. *Archives of Biochemistry and Biophysics* **268**: 93–99.

Rundle SJ, Zielinski RE. **1991**. Alterations in barley ribulose-1,5-bisphosphate carboxylase/oxygenase activase gene expression during development and in response to illumination. *Journal of Biological Chemistry* **266**: 14802–14807.

Salinas P, Fuentes D, Vidal E, Jordana X, Echeverria M, Holuigue L. **2006**. An Extensive Survey of CK2 α and β Subunits in Arabidopsis: Multiple Isoforms Exhibit Differential Subcellular Localization. *Plant and Cell Physiology* **47**: 1295–1308.

Salvucci ME, van de Loo FJ, Stecher D. **2003**. Two isoforms of Rubisco activase in cotton, the products of separate genes not alternative splicing. *Planta* **216**: 736–744.

Salvucci ME, Portis AR, Ogren WL. **1985**. A soluble chloroplast protein catalyzes ribulosebisphosphate carboxylase/oxygenase activation in vivo. *Photosynthesis Research* **7**: 193–201.

Salvucci ME, Portis AR, Ogren WL. **1986**. Light and CO_2 Response of Ribulose-1,5-Bisphosphate Carboxylase/Oxygenase Activation in *Arabidopsis* Leaves. *Plant Physiology* **80**: 655–659.

Salvucci ME, Werneke JM, Ogren WL, Portis AR. **1987**. Purification and Species Distribution of Rubisco Activase. *Plant Physiology* **84**: 930–936.

Samol I, Shapiguzov A, Ingelsson B, Fucile G, Crèvecoeur M, Vener A V., Rochaix JD, Goldschmidt-Clermont M. **2012**. Identification of a photosystem II phosphatase involved in light acclimation in Arabidopsis. *Plant Cell* **24**.

Sanchez de Jimenez E, Medrano L, Martinez-Barajas E. **1995**. Rubisco Activase, a Possible New Member of the Molecular Chaperone Family. *Biochemistry* **34**: 2826–2831.

Scafaro AP, Bautsoens N, den Boer B, Van Rie J, Gallé A. **2019**. A Conserved Sequence from Heat-Adapted Species Improves Rubisco Activase Thermostability in Wheat. *Plant Physiology* **181**: 43–54.

Schweer J, Türkeri H, Link B, Link G. **2010**. AtSIG6, a plastid sigma factor from Arabidopsis, reveals functional impact of cpCK2 phosphorylation. *The Plant Journal* **62**: 192–202.

Shivhare D, Mueller-Cajar O. **2017**. In Vitro Characterization of Thermostable CAM Rubisco Activase Reveals a Rubisco Interacting Surface Loop. *Plant Physiology* **174**: 1505–1516.

Soleh MA, Tanaka Y, Kim SY, Huber SC, Sakoda K, Shiraiwa T. **2017**. Identification of large variation in the photosynthetic induction response among 37 soybean [Glycine max (L.) Merr.] genotypes that is not correlated with steady-state photosynthetic capacity. *Photosynthesis Research* **131**: 305–315.

Soltis DE, Smith SA, Cellinese N, Wurdack KJ, Tank DC, Brockington SF, Refulio□Rodriguez NF, Walker JB, Moore MJ, Carlsward BS, *et al.* 2011. Angiosperm phylogeny: 17 genes, 640 taxa. *American Journal of Botany* **98**: 704–730.

Somerville CR, Portis AR, Ogren WL. **1982**. A Mutant of *Arabidopsis thaliana* Which Lacks Activation of RuBP Carboxylase *In Vivo*. *Plant Physiology* **70**: 381–387.

Stitt M, Quick WP, Schurr U, Schulze E-D, Rodermel SR, Bogorad L. **1991**. Decreased ribulose-1,5-bisphosphate carboxylase-oxygenase in transgenic tobacco transformed with□?antisense? rbcS. *Planta* **183**.

Stitt M, Schulze D. **1994**. Does Rubisco control the rate of photosynthesis and plant growth? An exercise in molecular ecophysiology. *Plant, Cell & Environment* **17**: 465–487.

Stotz M, Mueller-Cajar O, Ciniawsky S, Wendler P, Hartl FU, Bracher A, Hayer-Hartl M. **2011**. Structure of green-type Rubisco activase from tobacco. *Nature structural & molecular biology* **18**: 1366–70.

Tang H, Bowers JE, Wang X, Paterson AH. **2010**. Angiosperm genome comparisons reveal early polyploidy in the monocot lineage. *Proceedings of the National Academy of Sciences* **107**: 472–477.

To K-Y, Suen D-F, Chen S-CG. **1999**. Molecular characterization of ribulose-1,5-bisphosphate carboxylase/oxygenase activase in rice leaves. *Planta* **209**: 66–76.

Uhrig RG, Labandera A-M, Tang L-Y, Sieben NA, Goudreault M, Yeung E, Gingras A-C, Samuel MA, Moorhead GBG. **2017**. Activation of Mitochondrial Protein Phosphatase SLP2 by MIA40 Regulates Seed Germination. *Plant Physiology* **173**: 956–969.

Uhrig RG, Moorhead GB. **2011**. Two Ancient Bacterial-like PPP Family Phosphatases from Arabidopsis Are Highly Conserved Plant Proteins That Possess Unique Properties . *Plant Physiology* **157**: 1778–1792.

Werneke JM, Chatfield JM, Ogren WL. **1989**. Alternative mRNA splicing generates the two ribulosebisphosphate carboxylase/oxygenase activase polypeptides in spinach and Arabidopsis. *The Plant Cell* **1**: 815–825.

White-Gloria C, Johnson JJ, Marritt K, Kataya A, Vahab A, Moorhead GB. **2018**. Protein Kinases and Phosphatases of the Plastid and Their Potential Role in Starch Metabolism. *Frontiers in Plant Science* **9**.

Wijewardene I, Shen G, Zhang H. **2021**. Enhancing crop yield by using Rubisco activase to improve photosynthesis under elevated temperatures. *Stress Biology* **1**: 2.

Willems P, Horne A, Van Parys T, Goormachtig S, De Smet I, Botzki A, Van Breusegem F, Gevaert K. **2019**. The Plant <scp>PTM</scp> Viewer, a central resource for exploring plant protein modifications. *The Plant Journal* **99**: 752–762.

Willems P, Sterck L, Dard A, Huang J, De Smet I, Gevaert K, Van Breusegem F. **2024**. The Plant PTM Viewer 2.0: in-depth exploration of plant protein modification landscapes. *Journal of Experimental Botany*.

Yin Z, Meng F, Song H, Wang X, Xu X, Yu D. **2010**. Expression Quantitative Trait Loci Analysis of Two Genes Encoding Rubisco Activase in Soybean . *Plant Physiology* **152**: 1625–1637.

Zhang N, Kallis RP, Ewy RG, Portis AR. **2002**. Light modulation of Rubisco in *Arabidopsis* requires a capacity for redox regulation of the larger Rubisco activase isoform. *Proceedings of the National Academy of Sciences* **99**: 3330–3334.

Zhang N, Portis AR. **1999a**. Mechanism of light regulation of Rubisco: A specific role for the larger Rubisco activase isoform involving reductive activation by thioredoxin-f. *Proceedings of the National Academy of Sciences* **96**: 9438–9443.

Zhang N, Portis AR. **1999b**. Mechanism of light regulation of Rubisco: A specific role for the larger Rubisco activase isoform involving reductive activation by thioredoxin-f. *Proceedings of the National Academy of Sciences* **96**: 9438–9443.

Zhu X-G, de Sturler E, Long SP. **2007**. Optimizing the Distribution of Resources between Enzymes of Carbon Metabolism Can Dramatically Increase Photosynthetic Rate: A Numerical Simulation Using an Evolutionary Algorithm. *Plant Physiology* **145**: 513–526.

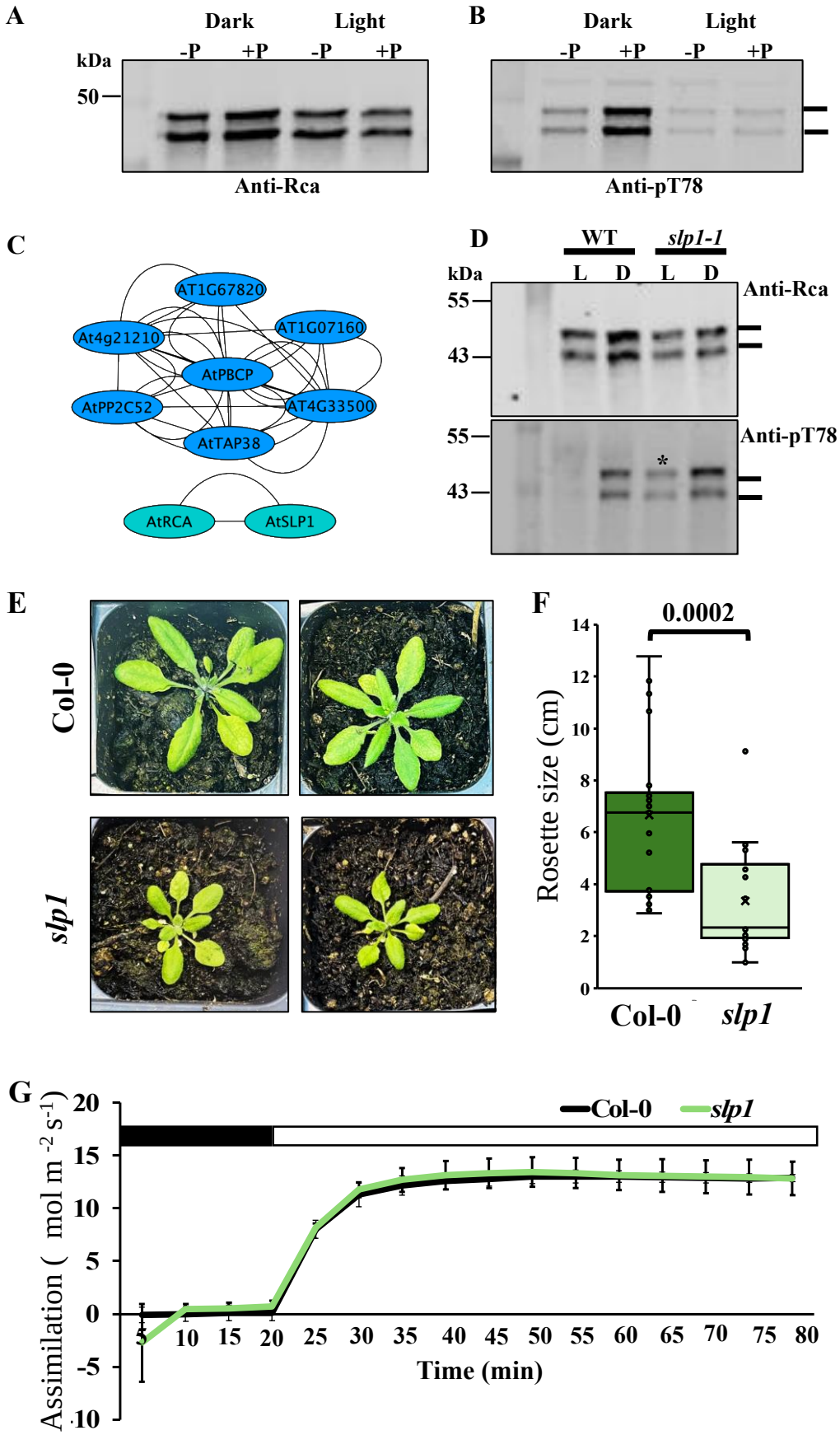
A
Dark
Light
-P
+P
-P
+P
kDa
50
Anti-Rca
B
Dark
Light
-P
+P
-P
+P
Anti-pT78
C
AT1G67820
At4g21210
AT1G07160
AtPBCP
AtPP2C52
AT4G33500
AtTAP38
AtRCA
AtSLP1
D
WT
slp1-1
kDa
L
D
L
D
55
43
Anti-Rca
55
43
Anti-pT78
*
E
Col-0
slp1
F
0.0002
Rosette size (cm)
14
12
10
8
6
4
2
0
Col-0
slp1
G
Col-0
slp1
Assimilation (mol m -2 s-1)
20
15
10
5
0
-5
-10
5
10
15
20
25
30
35
40
45
50
55
60
65
70
75
80
Time (min)

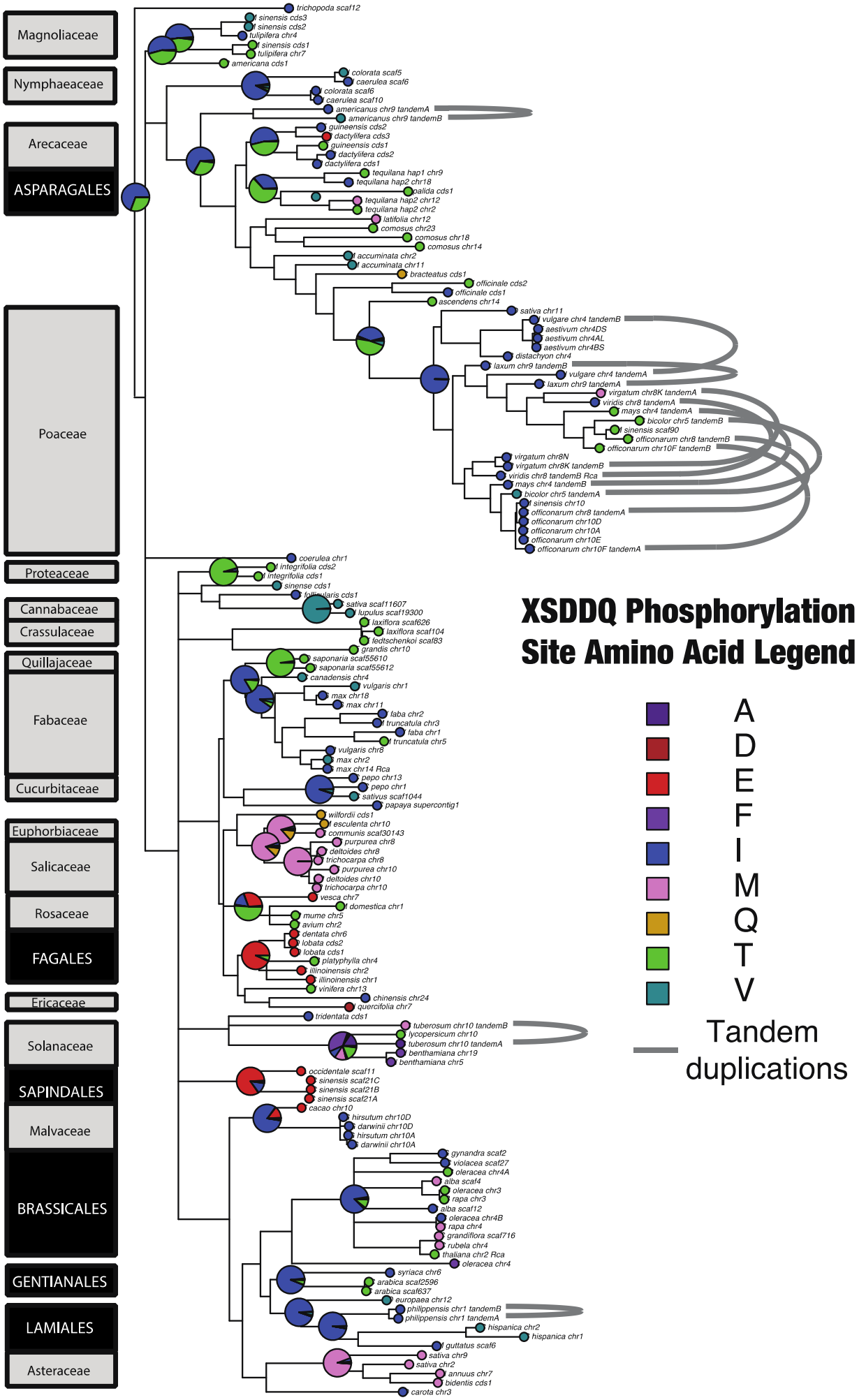
Magnoliaceae
Nymphaeaceae
Arecaceae
ASPARAGALES
Poaceae
Proteaceae
Cannabaceae
Crassulaceae
Quillajaceae
Fabaceae
Cucurbitaceae
Euphorbiaceae
Salicaceae
Rosaceae
FAGALES
Ericaceae
Solanaceae
SAPINDALES
Malvaceae
BRASSICALES
GENTIANALES
LAMIALES
Asteraceae
trichopoda scaf12
f sinensis cds3
f sinensis cds2
tulipifera chr4
f sinensis cds1
tulipifera chr7
americana cds1
colorata scaf5
caerulea scaf6
colorata scaf6
caerulea scaf10
americanus chr9 tandemA
americanus chr9 tandemB
guineensis cds2
dactylifera cds3
guineensis cds1
dactylifera cds2
dactylifera cds1
tequilana hap1 chr9
tequilana hap2 chr18
palida cds1
tequilana hap2 chr12
tequilana hap2 chr2
latifolia chr12
comosus chr23
comosus chr18
comosus chr14
f accuminata chr2
f accuminata chr11
bracteatus cds1
officinale cds2
officinale cds1
ascendens chr14
sativa chr11
vulgare chr4 tandemB
aestivum chr4DS
aestivum chr4AL
aestivum chr4BS
distachyon chr4
laxum chr9 tandemB
vulgare chr4 tandemA
laxum chr9 tandemA
virgatum chr8K tandemA
viridis chr8 tandemA
mays chr4 tandemA
bicolor chr5 tandemB
f sinensis scaf90
officonarum chr8 tandemB
officonarum chr10F tandemB
virgatum chr8N
virgatum chr8K tandemB
viridis chr8 tandemB Rca
mays chr4 tandemB
bicolor chr5 tandemA
f sinensis chr10
officonarum chr8 tandemA
officonarum chr10D
officonarum chr10A
officonarum chr10E
officonarum chr10F tandemA
coerulea chr1
f integrifolia cds2
f integrifolia cds1
sinense cds1
f foliularis cds1
sativa scaf11607
lupulus scaf19300
laxiflora scaf626
laxiflora scaf104
fedtschenkoi scaf83
grandis chr10
f saponaria scaf55610
f saponaria scaf55612
canadensis chr4
vulgaris chr1
max chr18
max chr11
faba chr2
f truncatula chr3
faba chr1
f truncatula chr5
vulgaris chr8
max chr2
max chr14 Rca
pepo chr13
pepo chr1
sativus scaf1044
papaya supercontig1
wilfordii cds1
f esculenta chr10
communis scaf30143
purpurea chr8
deltoides chr8
trichocarpa chr8
purpurea chr10
deltoides chr10
trichocarpa chr10
vesca chr7
f domestica chr1
mume chr5
avium chr2
dentata chr6
f lobata cds2
f lobata cds1
platyphylla chr4
illinoinensis chr2
illinoinensis chr1
vinifera chr13
chinensis chr24
quercifolia chr7
tridentata cds1
tuberosum chr10 tandemB
lycopersicum chr10
tuberosum chr10 tandemA
benthamiana chr19
benthamiana chr5
occidentale scaf11
sinensis scaf21C
sinensis scaf21B
sinensis scaf21A
cacao chr10
hirsutum chr10D
darwinii chr10D
hirsutum chr10A
darwinii chr10A
gynandra scaf2
violacea scaf27
oleracea chr4A
alba scaf4
oleracea chr3
rapa chr3
alba scaf12
oleracea chr4B
rapa chr4
grandiflora scaf716
rubela chr4
thaliana chr2 Rca
oleracea chr4
syriaca chr6
arabica scaf2596
arabica scaf637
europaea chr12
philippensis chr1 tandemB
philippensis chr1 tandemA
hispanica chr2
hispanica chr1
f guttatus scaf6
sativa chr9
sativa chr2
f annuus chr7
bidentis cds1
carota chr3
XSDDQ Phosphorylation Site Amino Acid Legend
A
D
E
F
I
M
Q
T
V
Tandem duplications

A

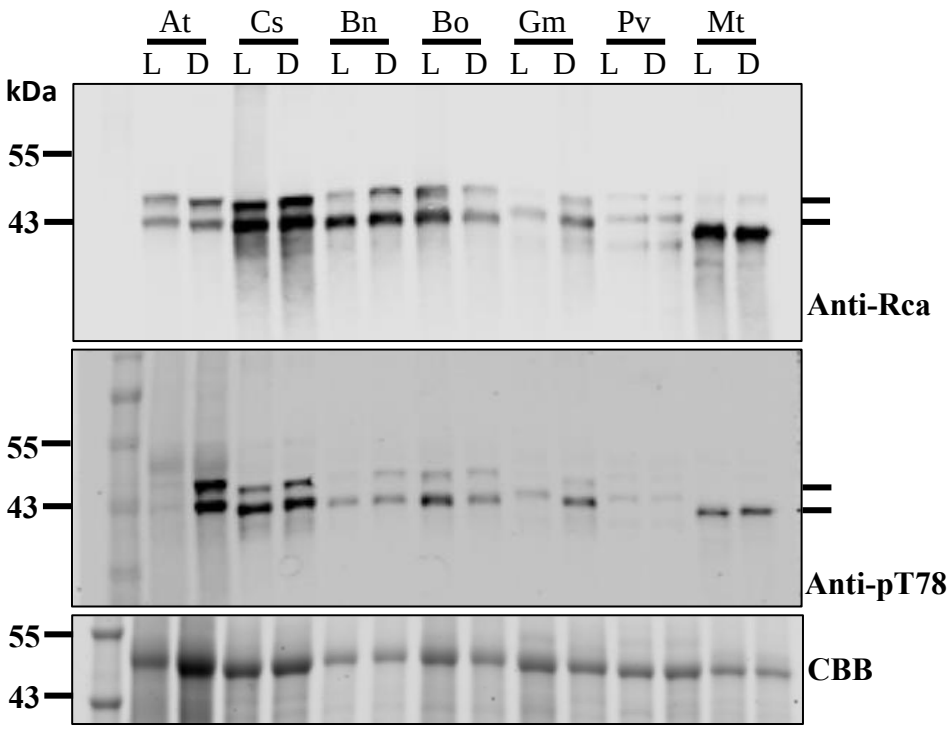
At
Cs
Bn
Bo
Gm
Pv
Mt
L D L D L D L D L D L D L D
kDa
55
43
Anti-Rca
55
43
Anti-pT78
55
43
CBB

B

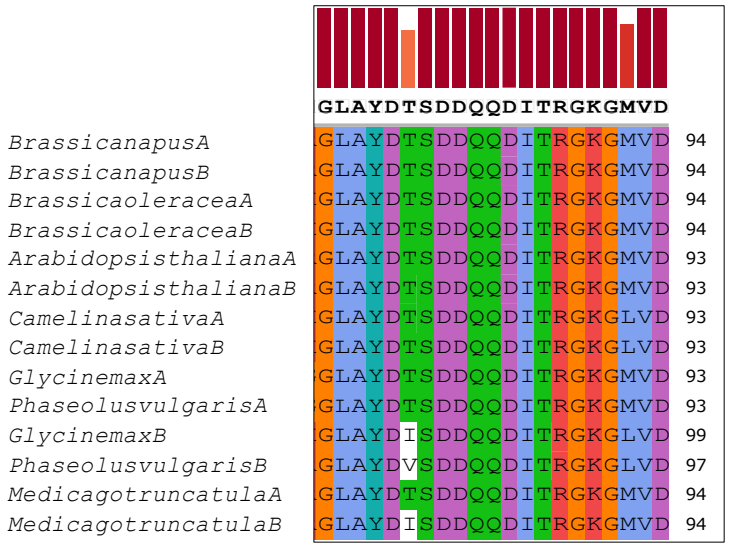
GLAYDTSDDQQDITRGKGMVD
BrassicanapusA GLAYDTSDDQQDITRGKGMVD 94
BrassicanapusB GLAYDTSDDQQDITRGKGMVD 94
BrassicaoleraceaA GLAYDTSDDQQDITRGKGMVD 94
BrassicaoleraceaB GLAYDTSDDQQDITRGKGMVD 94
ArabidopsisthalianaA GLAYDTSDDQQDITRGKGMVD 93
ArabidopsisthalianaB GLAYDTSDDQQDITRGKGMVD 93
CamelinasativaA GLAYDTSDDQQDITRGKGLVD 93
CamelinasativaB GLAYDTSDDQQDITRGKGLVD 93
GlycinemaxA GLAYDTSDDQQDITRGKGMVD 93
PhaseolusvulgarisA GLAYDTSDDQQDITRGKGMVD 93
GlycinemaxB GLAYDISDDQQDITRGKGLVD 99
PhaseolusvulgarisB GLAYDVSDDQQDITRGKGLVD 97
MedicagotruncatulaA GLAYDTSDDQQDITRGKGMVD 94
MedicagotruncatulaB GLAYDISDDQQDITRGKGMVD 94

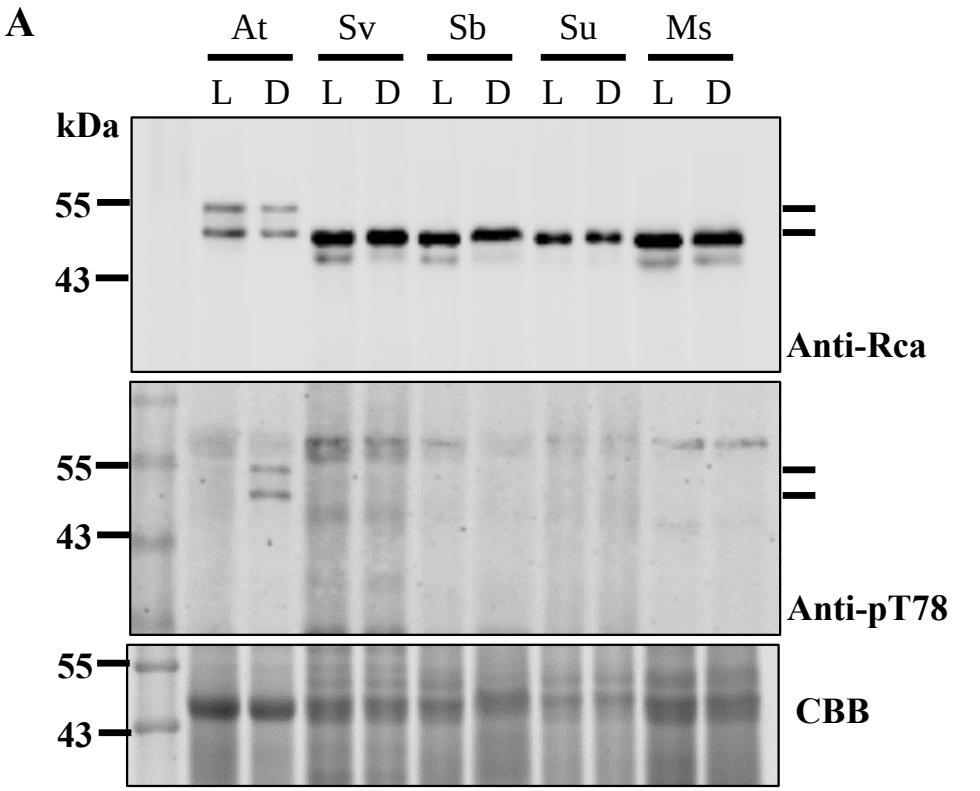
A
At
Sv
Sb
Su
Ms
L D L D L D L D L D
kDa
55
43
Anti-Rca
55
43
Anti-pT78
55
43
CBB

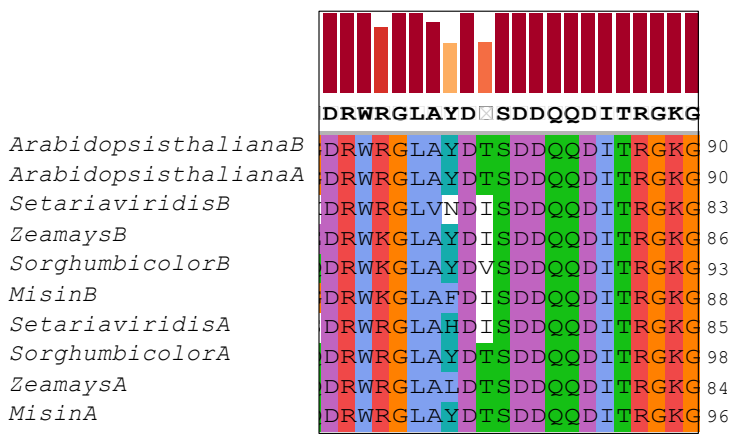
B
DRWRGLAYD SDDQQDITRGKG
ArabidopsisthalianaB DRWRGLAYDTSDDQQDITRGKG 90
ArabidopsisthalianaA DRWRGLAYDTSDDQQDITRGKG 90
SetariaviridisB DRWRGLVNDISDDQQDITRGKG 83
ZeamaysB DRWKGLAYDISDDQQDITRGKG 86
SorghumbicolorB DRWKGLAYDVSDDQQDITRGKG 93
MisinB DRWKGLAFDISDDQQDITRGKG 88
SetariaviridisA DRWRGLAHDISDDQQDITRGKG 85
SorghumbicolorA DRWRGLAYDTSDDQQDITRGKG 98
ZeamaysA DRWRGLALDTSDDQQDITRGKG 84
MisinA DRWRGLAYDTSDDQQDITRGKG 96

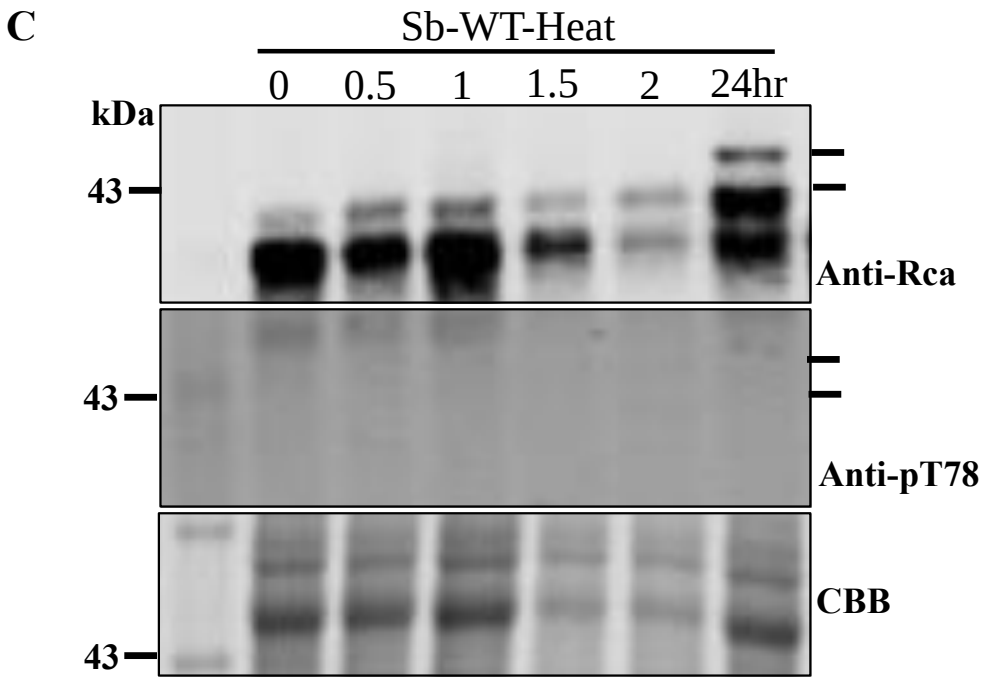
C
Sb-WT-Heat
0 0.5 1 1.5 2 24hr
kDa
43
Anti-Rca
43
Anti-pT78
CBB
43

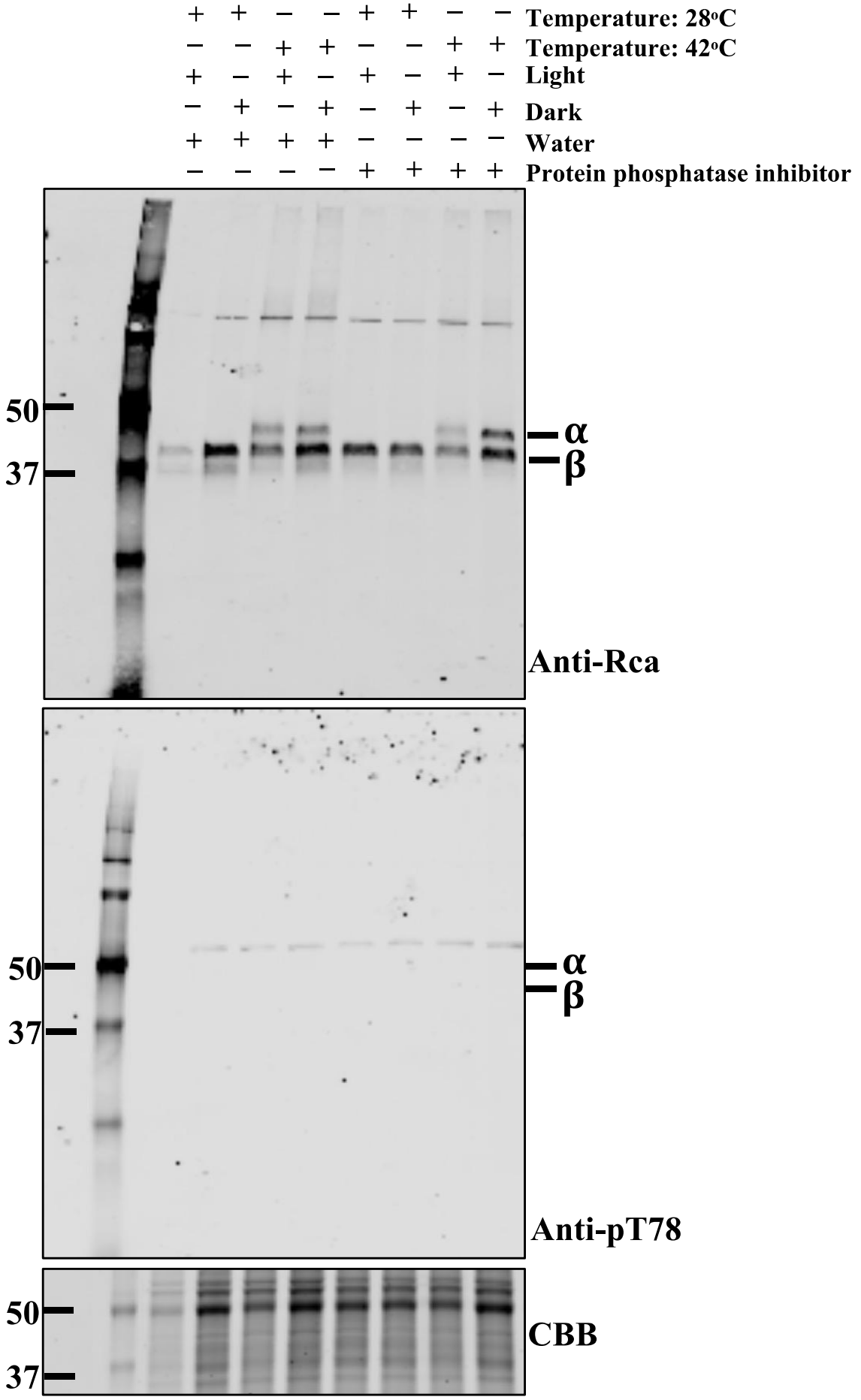
+ + − − + + − − Temperature: 28°C
− − + + − − + + Temperature: 42°C
+ − + − + − + − Light
− + − + − + − + Dark
+ + + + − − − − Water
− − − − + + + + Protein phosphatase inhibitor
50
37
α
β
Anti-Rca
50
37
α
β
Anti-pT78
50
37
CBB